Flutter Characteristics ofAircraft Wing Considering Control Surface and Actuator Dynamics with Friction Nonlinearity

Seung-Jun Lee* and In Lee***
Department of Aerospace Engineering
Korea Advanced Institute of Science and Technology, Daejeon, Korea

Won-Ho Shin**
Samsung Electro-Mechanics, Suwon, Korea

Abstract

Whenever the hinge axis of aircraft wing rotates, its stiffness varies. Also, there are nonlinearities in the connection of the actuator and the hinge axis, and it is necessary to inspect the coupled effects between the actuator dynamics and the hinge nonlinearity. Nonlinear aeroelastic characteristics are investigated by using the iterative V-g method. Time domain analyses are also performed by using Karpel's minimum state approximation technique. The doublet hybrid method(DHM) is used to calculate the unsteady aerodynamic forces in subsonic regions. Structural nonlinearity located in the load links of the actuator is assumed to be friction. The friction nonlinearity of an actuator is identified by using the describing function technique. The nonlinear flutter analyses have shown that the flutter characteristics significantly depends on the structural nonlinearity as well as the dynamic stiffness of an actuator. Therefore, the dynamic stiffness of an actuator as well as the nonlinear effect of hinge axis are important factors to determine the flutter stability.

Key Word : Dynamic Stiffness, Friction, Nonlinearity, Flutter, DHM

Introduction

Aeroelasticity is the research field of investigating the interacting effects between the structural dynamics and aerodynamics. It means that the vehicle structure itself may be unstable when the aerodynamics is coupled. That phenomenon resultes from the change of stiffness of the system. It may cause failure of vehicle structure or degradation of control performance. In addition, the light-weight structure and high specific stiffness material like composite structure is taking an important part in modern aerospace industry. It can increase the static stability, but can decrease the dynamic stability. Accordingly, aeroelastic phenomena such as divergence, flutter, and gust response and so on, have become significant issues in flight vehicle design. It is needed to predict aeroelastic behaviors precisely to ensure the flight stability region.

In recently developed aircrafts, the control systems of wings have become complex for better flight performance. As actuators become more advanced, the effects of actuator dynamics on aeroelasticity of flight vehicles become more significant. Hence, the structural dynamics,

* Research Assistant
** Researcher, Samsung Electro-Mechanics
*** President, KSAS & Professor, Aerospace Engineering Dept., KAIST
E-mail : inlee@kaist.ac.kr Tel : 82-42-869-3717 Fax : 82-42-869-3710

aerodynamics, and the control system interacting problem should be considered for the design of aircraft wing. For the control surface of wing, there is an additional degree of freedom and it can produce some nonlinear responses. The nonlinearities can be classified into the form of freeplay, friction, backlash, and so on. It can cause the limit cycle oscillation(LCO) phenomenon. Especially, for a wing having control surface and an actuator, there can exist nonlinearity such as friction in hinge axis, in other words, the load link of an actuator. Therefore, to consider the nonlinear servo-motor motion, the nonlinear effect should be resolved into the actuator dynamics equations.

The nonlinear flutter phenomena due to the geometrical nonlinearities have been studied by many researchers. Woolston et al. performed experiment for the typical section wing having nonlinearities, and found that the LCO occurred at the lower velocity range than the linear case[1]. Laurenson and Trn studied the freeplay nonlinearity for a tail wing by using describing function and subsonic quasi-steady aerodynamics[2]. McIntosh et al. performed experimental and theoretical studies for nonlinear flutter of a typical section wing with nonlinearity, and they observed LCO and flutter[3]. Karpel studied the nonlinear behavior of wing/store model by using the minimum state approximation method and the ficticious mass method[4]. Conner et al. performed experiments and finite elements analyses for flapped wing with freeplay[5]. Bae et al. studied the subsonic nonlinear flutter phenomena for wings having control surface in frequency and time domains[6]. Besides, several researches about actuator modeling have been performed. Dulger and Uyan developed the mathematical model for no-electric-discharge servo motor[7]. Torfs and Schutter constituted the mathematical model of the motion of the link due to the velocity control actuator[8]. Ebrahimi and Whalley modeled and analyzed the backlash, friction, and preload nonlinearity of an actuator[9]. Guesalage performed the modeling of the dynamic characteristics of a position servo motor[10]. Tavakoli et al. clarified that the transmission error is one of the biggest problems inducing vibration and noise[11]. Paek and Lee performed a flutter analysis for a launch vehicle control surface with control actuators and investigated the effect of the sweep angle on the flutter characteristics with dynamic stiffness[12].

Many researches have been performed for nonlinear flutter. However, nonlinear flutter analyses considering the structural nonlinearity of an actuator have not yet been performed. In this paper, the nonlinear aeroelastic characteristics of a wing with an actuator are investigated with consideration of actuator nonlinearities as well as the actuator dynamics. Actuator nonlinearities including friction are present in the actuator, and the transfer function of the actuator is obtained via a rational function type comprised of system coefficients. The finite element method is used for the free vibration analysis, and the DHM and DPM are used for the computation of subsonic unsteady aerodynamic forces. The fictitious mass method is used to reduce the computational efforts.

Theoretical Backgrounds

Actuator Governing Equation

Figure 1 shows that the free body diagram of the actuator which consists of an electric motor, gears, and load links. The governing equations of the actuator can be obtained using the Newton's 2nd law at each point. The equation of motion can be represented as the combination of mass, damping, and stiffness of a motor at point A, B, C, and D[13].

$$J_m\ddot{\theta}_m + C_m\dot{\theta}_m + K_m\theta_m = T - T_1, \tag{1}$$

$$J_1\frac{\ddot{\theta}_m}{N_1} = N_1T_1 - c_1\left(\frac{\dot{\theta}_m}{N_1} - \dot{\theta}_n\right) - k_1\left(\frac{\theta_m}{N_1} - \theta_n\right), \tag{2}$$

$$J_2\ddot{\theta}_n = -c_1\left(\dot{\theta}_n - \frac{\dot{\theta}_m}{N_1}\right) - k_1\left(\theta_n - \frac{\theta_m}{N_1}\right) - \frac{T_L}{N_2}, \tag{3}$$

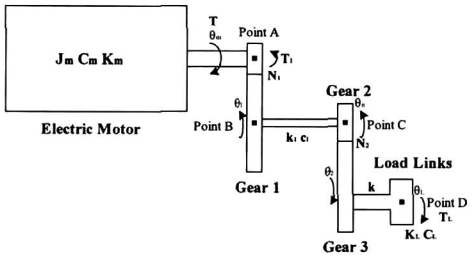

Fig. 1. The free body diagram of the gear systems

$$J_L\ddot{\theta}_L + C_L\dot{\theta}_L + K_L\theta_L = T_L. \tag{4}$$

The symbols, J, C, K, T, represents the moment of inertia, damping coefficient, stiffness, and torque, respectively. And the subscript m, 1, 2, L shows an electric motor, gear1, gear2, and a load link, respectively. Also, N_1 means the speed reduction rate of between the electric motor and gear1 and N_2 means the speed reduction rate of between the gear2 and gear3.

There is transmission error β between gear 3 and the load axis. The transmission torque can be represented as the product between stiffness and transmission error,

$$T_L = k\beta. \tag{5}$$

In this paper, the F-5 wing scale-down model which is widely used for aeroelastic analyses, is adopted, and the actuator is LC38RM-009-200 electric motor, which has 6 order of J_m. Therefore, it is assumed that the moments of inertia of gears are negligibly small and solving equations (1)-(5), the transfer function of the actuator with transmission errors finally can be represented as a function of displacements of each load axis and input torque.

$$\frac{T(s)}{\theta_L(s)} = N_1\left(J_m s^2 + C_m s + K_m\right)\left[\left\{\frac{1}{N_2\left(k_1 + c_1 s\right)} + \frac{1}{k}\right\}\times \left(J_L s^2 + C_L s + K_L\right) + N_2\right]\frac{J_L s^2 + C_L s + K_L}{N_1 N_2}. \tag{6}$$

Friction Nonlinearity Modeling

Actuators may include several structural nonlinearities, such as friction among the gears, freeplay of the load links, and transmission errors within the electric motor, gears, and load links. Such actuator nonlinearities may affect seriously the dynamic characteristics of a given actuator. If the nonlinearites appear in the aeroelastic analyses, it may cause difficulty in analyzing the system. Most mechanical systems have the low pass filter characteristics. It means that when an arbitrary sinusoidal wave is given, the higher harmonic terms will be vanished because of the low-pass filter feature. Therefore, the system can be identified by the basic frequencies, that is, the nonlinearity can be approximated by the combination of simple harmonic motions which have the same frequency as the input wave. The input wave and the restoring force can be written as

$$x = X\sin\omega t, \tag{7}$$

$$f(t) = a_0 + a_1\cos\omega t + b_1\sin\omega t. \tag{8}$$

Figure 2 shows the simplified behavior of friction.

The nonlinear characteristics is concentrated on the origin. Except for the nonlinear point, the overall structural behavior is assumed to be linear with stiffness, K, and symmetry about the

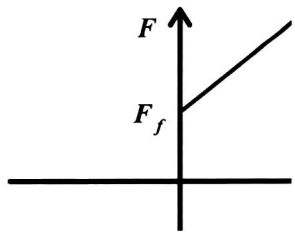

Fig. 2. The simplified friction nonlinearity model

nonlinear point. The friction nonlinearity has the following relationship between displacement and restoring force.

$$F(x)=\begin{cases} Kx+F_f & at \quad x>0 \\ Kx-F_f & at \quad x<0 \end{cases} \tag{9}$$

Consequently, the equivalent stiffness of a nonlinear spring can be obtained using the general describing function method[14] and can be written as

$$K_{eq,friction}(X)=\frac{4F_f}{\pi X}+k \tag{10}$$

Aeroelastic Equations

The aeroelastic equations of the wing with concentrated structural nonlinearity, such as freeplay, can be written as

$$\mathbf{M}\ddot{\mathbf{u}}+\mathbf{C}\dot{\mathbf{u}}+\mathbf{K}_u(\omega,\mathbf{u})\mathbf{u}=\mathbf{F}(t,\mathbf{u},\dot{\mathbf{u}}) \tag{11}$$

where, **M**, **C**, and **u** are the mass matrix, damping matrix and displacement vector, respectively. In addition, **F** is the unsteady aerodynamic force and $\mathbf{K}_u$ is the nonlinear stiffness matrix. The nonlinear stiffness matrix is divided into linear and nonlinear terms, which can be written as

$$\mathbf{K}_u(\omega,\mathbf{u})\mathbf{u}=\mathbf{K}(\omega)\mathbf{u}+f(\omega,\mathbf{u}) \tag{12}$$

where $\mathbf{K}(\omega)$ is a dynamic stiffness matrix, and $f(\omega,\mathbf{u})$ is the restoring force vector. In an aeroelastic system with structural nonlinearity and dynamic stiffness, structural properties vary with the behavior of system. Hence, the aeroelastic results may be inaccurate if the constant modal coordinate of the nominal model is used to reduce the computational time. Also, it takes too much time to redefine the modal coordinates of the aeroelastic system as the structural properties vary. For these reasons, the fictitious mass method is used to improve accuracy and computational time while using generalized modal coordinates.

The fictitious mass is added to interface coordinates between the actuator and structure. The equation of motion with fictitious mass, $\mathbf{M}_F$, can be rewritten as

$$(\mathbf{M}+\mathbf{M}_F)\ddot{\mathbf{u}}+\mathbf{C}\dot{\mathbf{u}}+\mathbf{K}\mathbf{u}=\mathbf{F}(t,\mathbf{u},\dot{\mathbf{u}}). \tag{13}$$

The eigenvector and eigenvalue matrices are obtained solving the eigenvalue problem of equation (13). When the modal matrix $\mathbf{\Phi}_F$ of the fictitious mass (FM) model is used, the structural displacement vector can be transformed into modal coordinates as follows

$$\mathbf{u}=\mathbf{\Phi}_F\boldsymbol{\eta} \tag{14}$$

On the other hand, the governing equation of the real structure having $\Delta\mathbf{K}(\omega,\mathbf{u})$, induced by actuator nonlinearity and dynamics, is written as

$$\mathbf{M}\ddot{\mathbf{u}} + \mathbf{C}\dot{\mathbf{u}} + (\mathbf{K} + \Delta\mathbf{K})\mathbf{u} = \mathbf{F}(t, \mathbf{u}, \dot{\mathbf{u}}). \tag{15}$$

Therefore, equation (15) can be rewritten as

$$(\bar{\mathbf{M}} - \boldsymbol{\Phi}_F^T \mathbf{M}_F \boldsymbol{\Phi}_F)\ddot{\boldsymbol{\eta}} + \bar{\mathbf{C}}\dot{\boldsymbol{\eta}} + (\bar{\mathbf{K}} + \boldsymbol{\Phi}_F^T \Delta\mathbf{K}(\omega, \mathbf{u})\boldsymbol{\Phi}_F)\boldsymbol{\eta} = \mathbf{q}\bar{\mathbf{Q}}\boldsymbol{\eta} - \boldsymbol{\Phi}_F^T f(\omega, \mathbf{u}). \tag{16}$$

Although $\Delta\mathbf{K}(\omega, \mathbf{u})$ has various values, $\boldsymbol{\Phi}_F$ is consistently used to construct the generalized coordinate. It is not necessary to perform the free vibration analysis again when the structure changes occur. The fictitious mass method is an efficient and simple method to perform the aeroelastic analysis for the nonlinear structures.

Results

Wing Details

The wing model is Nortsshrop F-5 fighter wing model with a control surface. The schematic diagram of the wing model is shown in Figure 3. The properies are written in Table 1.

The free vibration analysis is performed by using MSC/NASTRAN. The lifting surface and control surface are constituted by 9-node plate elements, and the joining nodes at hinge axis are linked by multi-point constraint(MPC) by which the rigid body mode is embodied. Torsional spring is added to realize the rotational stiffness. The root chord is clamped except for the part of control surface. Figure 4 represents the first six modes of the wing.

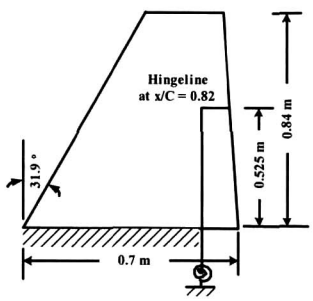

Fig. 3. Geometric configuration of fighter wing with flap

Table 1. Properties of F-5 flapped wing

Parameters	Value	Units
Material	Aluminum	
E	70.97	*GPa*
ρ	2900	kg/m^3
ν	0.33	

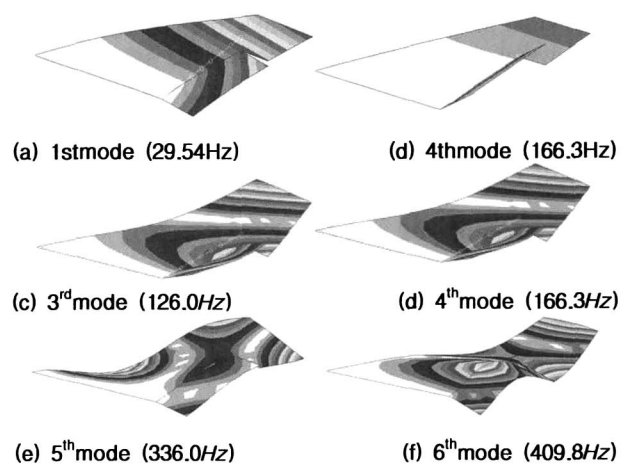

Fig. 4. Natural mode shapes of fighter wing with flap ($K_l = 1.5\times10^6 Nmm/rad$)

The 1st mode is first bending mode, the 2nd mode is control surface pitching mode, the 3rd mode is first torsion mode, the 4th mode is bending-torsion mode, the 5th mode is second bending mode, and the 6th mode is third bending mode.

Actuator Details

The actuator is LC38RM-009-200 electric motor made by Copal Company. The electric motor used in this study has static friction of 0.0028 N/m and an armature resistance of 9.52 Ω. Additionally, the motor torque constant, *back -emf*, and motor inertia are 0.039 N·m/A, 0.055 V/rad·sec, and 4.5×10-6 kg·m^2, respectively.

From the equations (10) and (6), the equivalent stiffness of friction and the nonlinear dynamic stiffness were plotted. Figure 5 shows the equivalent stiffness ratio with respect to the degree displacement. Because of the friction characteristics in Figure 5, the equivalent stiffness ratio is increased to infinity when the displacement is near zero. The friction equivalent stiffness also approaches to the linear hinge stiffness when the nondimensional displacement increases. Figure 6 shows the nonlinear dynamic stiffness and phase variation with respect to the frequency. When the amplitude has become 2 deg., the dynamic stiffness has been changed significantly, but the location of the poles has not been changed. Therefore, it is found that the friction force only affects the magnitude of the dynamic stiffness.

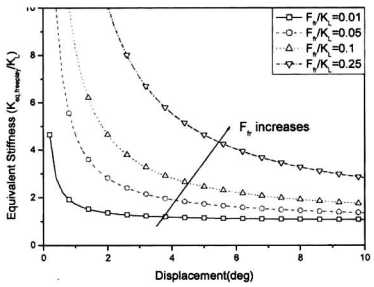

Fig. 5. Equivalent stiffness of friction

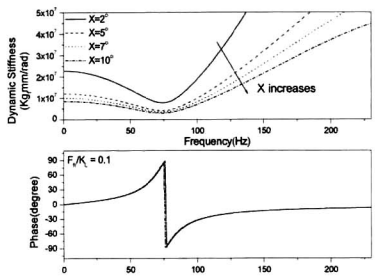

Fig. 6. Dynamic stiffness of friction

Linear Aeroelastic Results

Thehe unsteady aerodynamics were computed using the DHM for F-5 wing model with control surface in subsonic region, and the aeroelastic analysis is performed.

The 10×16 aerodynamic grid is constructed. The subsonic Mach number, 0.7, is selected and 10 structural modes are used. To find the flutter point in frequency domain, V-g method is used. Figures 7 shows the V-g and V-f plots at Mach number 0.7. When Mach number is 0.7, the flutter speed is 706.9 m/s and the flutter frequency is 112.0 Hz. If Mach number is 2.0, the flutter speed is 257.1 m/s and the flutter frequency is 98.48 Hz.

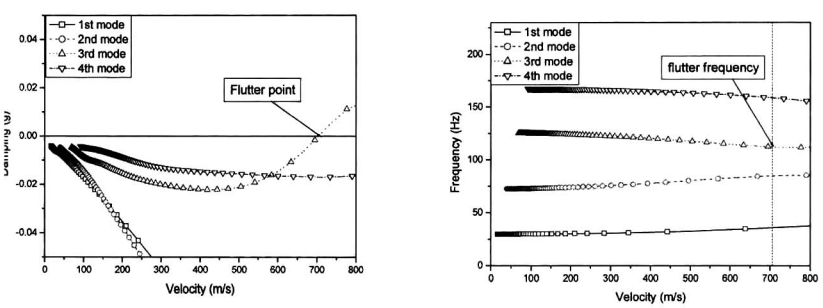

(a) V-g plot (b) V-f plot

Fig. 7. Linear aeroelastic results in frequency domain

Nonlinear Aeroelastic Results

Firstly, the graphs in Figure 8 represent the LCO responses. Let's define the friction coefficient, $\mathbf{a_{fr}}$, as $\mathbf{F_{fr}/K_L}$. When $\mathbf{F_{fr}}$ increases, the equivalent stiffness is increased. And it influences the flutter dynamic pressure. Mach number is 0.7, and the friction coefficient is set to vary from 0.01 to 0.25. Figure 8 shows only the cases in which $\mathbf{a_{fr}}$ is equal to 0.01 and 0.05, respectively. As already seen in Figure 5, the high stiffness ratio at the near zero displacement region causes the huge variance of flutter boundary from the linear one. When the friction coefficient increases, the equivalent stiffness is settled in higher value than the lower coefficient in Figure 5. This change finally influences the nonlinear flutter boundary.

In addition, the aeroelastic system combined with the actuator dynamics is analyzed. The results show that the nonlinear system behaves as if it is the linear system in this case.

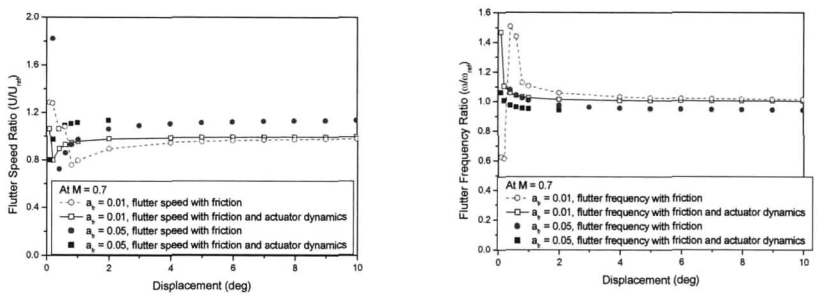

(a) flutter speed ratio (b) flutter frequency ratio

Fig. 8. Nonlinear flutter analysis with friction and actuator dynamics

Conclusions

In this study, the influences of actuator nonlinearities included in the actuator dynamics on aeroelastic characteristics have been investigated by using V-g method and iterative V-g methods in subsonic flows. The unsteady aerodynamic force coefficients have been calculated by using DHM based on a panel method. The changes of actuator dynamics induced by actuator nonlinearities were investigated. The results show that the friction can affect the magnitude of dynamic stiffness. LCOs were observed both below and above the linear flutter speed, and the LCO characteristics of the aeroelastic system are significantly dependent on actuator nonlinearity. The aeroelastic boundary may decrease due to the actuator nonlinearities as compared with a linear case. Thus, the actuator nonlinearities may play a significant role in the nonlinear flutter characteristics of an aeroelastic system. The results also indicate that it is necessary to consider the actuator dynamics at the design stage to prevent aeroelastic instabilities of aircrafts or missiles.

Acknowledgement

This research is supported by the FVRC(flight vehicle research center) by the Agency for Defence Development, Korea. Authors are grateful for their supports.

References

1. Woolston, D. S., Runyan, H. W. and Andrews, R. E., 1957, "Some Effects of System Nonlinearities in the Problem of Aircraft Flutter", NACA TN 3539.

2. Laurenson, R. M. and R. M. Trn, 1980, "Flutter Analysis of Missile Control Surfaces Containg Structural Nonlinearites", *AIAA Journal,* Vol. 18, No. 10, pp. 1245-1251.

3. McIntosh, S. C., Reed R. E. Jr. and Rodden, W. P., 1981, "Experimental and Theoretical

Study of Nonlinear Flutter", *Journal of Aircraft*, Vol. 18, No. 12, pp. 1057-1063.

4. Karpel, M., 1982, "Design for Active Flutter Suppression and Gust Alleviation Using State-Space Aeroelastic Modeling", *Journal of Aircraft*, Vol. 19, No. 3, pp. 221-227.

5. Conner, M. D., Tang, D. M., Dowell, E. H. and Virgin, L. N., 1997, "Nonlinear Behavior of a Typical Airfoil Section with Control Surface Freeplay: A Numerical and Experimental Study", *Journal of Fluids and Structures*, Vol. 11, No. 1, pp. 89-110.

6. Bae, J. S., Yang, S. M. and Lee, I., 2002, "Linear and Nonlinear Aeroelastic Analysis of a Fighter-type Wing with Control Surface", *Journal of Aircraft*, Vol. 39, No. 4, pp. 697-708.

7. Dulger, L. C. and Uyan, S., 1997, "Modeling, Simulation and Control of a Four-Bar Mechanism with a Brushless Servo Motor", *Mechatronics*, Vol. 7, No. 4, pp. 369-383.

8. Torfs, D. and Schutter, J. D., 1995", Modeling and Control of a Flexible One-Link Robot Driven by a Velocity Controlled Actuator", *Mechanical Systems and Signal Processing*, Vol. 9, No. 1, pp. 15-29.

9. Ebrahimi, M. and Whalley, R., 2000, "Analysis, Modeling and Simulation of Stiffness in Machine Tool Drives", *Computers & Industrial Engineering,* Vol. 38, No. 1, pp. 93-105.

10. Guesalaga, A., 2004, "Modelling End-of-roll Dynamics in Positioning Servos," *Control Engineering Practice*, Vol. 12, No. 2, pp. 217-224.

11. Tavakoli, M. S. and Houser, D. R., 1986, "Optimum Profile Modifications for the Minimization of Static Transmission Errors of Spur Gears", *ASME, Journal of Engineering for Industry,* Vol. 108, No. 1, pp. 86-95.

12. Paek, S. K., and Lee, I, "Flutter analysis for control surface of launch vehicle with dynamic stiffness", *Computers & Structures*, Vol. 60, No. 4, pp. 593-599.

13. Shin, W. H., 2007, "Aeroservoelastic Analysis of Missile Fin Considering Structural Nonlinearity", Ph. D. Thesis, Department of Aerospace Engineering, Korea Advanced Institute of Science and Technology.

14. Gelb A. and Vander Velde, W. E., 1968, "Multiple-input describing functions and nonlinear system design", McGraw-Hill, Inc.